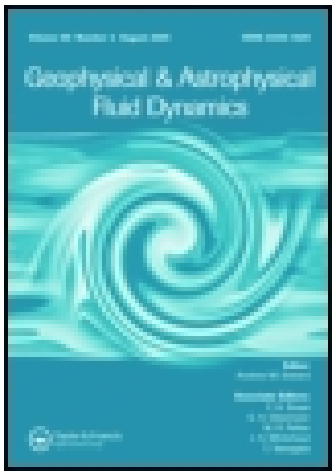

Geophysical Fluid Dynamics
Publication details, including instructions for authors and subscription information:
http://www.tandfonline.com/loi/ggaf19

Salt fingers in a steady shear flow

P. F. Linden [a]
[a] Department of Applied Mathematics and Theoretical Physics , University of Cambridge
Published online: 13 Oct 2008.

To cite this article: P. F. Linden (1974) Salt fingers in a steady shear flow, Geophysical Fluid Dynamics, 6:1, 1-27, DOI: 10.1080/03091927409365785

To link to this article: http://dx.doi.org/10.1080/03091927409365785

Geophysical Fluid Dynamics, 1974, Vol. 6, pp. 1–27

Printed in Great Britain

Salt Fingers in a Steady Shear Flow

P. F. LINDEN

Department of Applied Mathematics and Theoretical Physics
University of Cambridge

(*Received February 16, 1973*)

Salt fingers in a steady shear flow are examined both theoretically and in the laboratory. Linear stability analysis for small, uniform shears shows that all modes with a component of the shear normal to their wavecrests are stabilized by the shear, and consequently the preferred mode of instability is that of two-dimensional sheets aligned downshear. An examination of the energy equation shows that the main stabilizing force comes from the tilt of the modes by the component of the shear normal to their wavecrest. These two-dimensional sheets are found to equilibrate at finite amplitude in a manner analogous to rolls in thermal convection. The experimental study revealed that these two-dimensional sheets are indeed found in the laboratory, and measurements of fluxes indicate that they are almost equally efficient as salt fingers in transporting heat and salt vertically.

1. Introduction

In oceanographic situations where salt fingers may be an important mechanism for the transport of heat and salt in the vertical, velocity shears may also be present. For example, in the region where the Mediterranean water flows into the Atlantic (see Tait & Howe, 1968), it seems likely (although there is no direct evidence yet) that the bulk motion of the water masses may produce vertical shears in the microstructure. In an earlier paper Linden (1971) showed that turbulent motions imposed on salt fingers had a disruptive effect and inhibited the vertical salt transport. Can steady velocity shears have a similar effect? Before the role of salt fingers in the ocean, and in other contexts, can be properly evaluated it is necessary to determine the effects of a steady shear on their structure and on the vertical transports of heat and salt. This paper attempts to answer this question by investigating both theoretically and experimentally the effect of a steady velocity shear on the fingers.

Salt finger convection is analogous to Bénard convection in that the kinetic energy of the motions is obtained from the potential energy stored in the unstable distribution of a stratifying component. It is possible then, on the

basis of a linear stability analysis (see Baines & Gill, 1969) to define an "effective Rayleigh number" R^* which must exceed a critical value before convection can occur. R^* is related to the Rayleigh numbers R_S and R_T of the two components S and T which contribute to the density stratification by the equation $R^* = R_S - \tau R_T$, where $\tau = \kappa_S/\kappa_T$ is the ratio of the molecular diffusion coefficients of S and T. It will be seen that a steady shear will effect the salt fingers in a manner analogous to the effects of shear on Benard convection. Therefore, it is worth mentioning the results of investigations on Benard convection in a shear flow before proceeding to the double-diffusive case.

In 1928 Jeffreys suggested that a steady shear in an unstably stratified fluid stabilizes all perturbations except the one mode of infinite length in the direction of the shear flow, and hence that the convective disturbance takes the form of rolls aligned along the direction of the shear. Laboratory studies by Graham (1934) and Chandra (1938) and more recently by Ingersoll (1966a) have supported Jeffrey's idea. A number of theoretical studies by Kuo (1963), Asai (1964, 1970a, b), Deardorff (1965), Gallagher & Mercer (1965) and Ingersoll (1966b) have also confirmed Jeffrey's conclusion. These later studies have provided neutral stability curves for various ranges of the non-dimensional parameters of the problem namely the Reynolds number, the Rayleigh number and the Prandtl number. Further Asai (1970a) has shown numerically that, for a stationary disturbance in a constant shear, the mode transverse to the basic flow transfers momentum upwards against the shear, whereas for the mode aligned along the shear the kinetic energy of the mean flow is converted into perturbation kinetic energy by transfer of horizontal momentum downwards. He further showed (1970b) that a variable shear effects the instability in a qualitatively similar way to constant shear.

On the basis of the thermal analogy it is of interest to discover whether salt fingers are converted into two-dimensional sheets by the shear, and how the vertical fluxes of heat and salt are changed by the shear. In order to answer these questions the remainder of this paper is divided into the following sections. In §2 the linear stability of salt finger modes in a uniform shear, and the momentum transport of the various modes, is discussed. Attention is given to the case where the shear is small; the interface will not be unstable to shear instability. It is found that the preferred mode of instability is in the form of two-dimensional sheets aligned in the direction of the mean shear. In §3 it is shown that these sheets equilibrate at small, but finite, amplitude in a manner analogous to the two-dimensional rolls found in thermal convection. The remainder of the paper is concerned with the experimental study of sheared salt fingers. Particular attention is paid to the horizontal structure and the vertical fluxes of S and T through the fingers. In order that the theory be kept general the two components contributing to the density distribution

will be referred to as S and T with, by definition, $\tau = \kappa_S/\kappa_T < 1$. The experiments are carried out using heat-salt and salt-sugar fingers, where $\tau \approx 0.01$ and 0.35, respectively.

2. Linear Stability Analysis

(a) *The equations of motion*

The stability of double-diffusive convection in a uniform steady shear flow is considered. The fluid is assumed to flow between free, conducting boundaries at $z = \pm d/2$, where Oz is the vertical axis. The upper boundary is maintained at concentration values ΔS and ΔT relative to the lower boundary; ΔS and ΔT are both positive for salt finger convection and attention will be restricted to this case throughout. Free, conducting boundaries at $z = \pm d/2$ are chosen for convenience, and they seem to be the most relevant ones for application to the laboratory and oceanic cases if the edges of the convecting layers on either side of the salt finger interface represent these boundaries; in that case ΔS and ΔT would be identified with the differences in S and T between these layers.

A linear equation of state

$$\rho = \rho_0(1-\alpha T+\beta S),$$

where α and β are the coefficients of expansion due to T and S, respectively is assumed. The molecular properties of the system viz ν (the kinematic viscosity), κ_S, κ_T, α and β are assumed to be constants. The non-dimensional, Boussinesq, linearized equations of momentum, heat and salt conservation may be written in the form

$$\left[\frac{1}{\sigma}\left(\frac{\partial}{\partial t}+\sigma Re U(z)\frac{\partial}{\partial x}\right)-\nabla^2\right]\nabla^2 w+\frac{Re}{\sigma}\frac{d^2U(z)}{dz^2}\frac{\partial w}{\partial x}-R_T\nabla_H^2 T+R_S\nabla_H^2 S=0,$$

$$\left[\frac{\partial}{\partial t}+\sigma Re U(z)\frac{\partial}{\partial x}-\nabla^2\right]T+w=0,$$

$$\left[\frac{\partial}{\partial t}+\sigma Re U(z)\frac{\partial}{\partial x}-\tau\nabla^2\right]S+w=0, \tag{2.1}$$

where w is the vertical velocity.

The boundary conditions at $z = \pm\frac{1}{2}$ are

$$\begin{aligned} &\text{free:} && w = w_{zz} = 0 \\ &\text{conducting:} && T = S = 0. \end{aligned} \tag{2.2}$$

The non-dimensional parameters describing the flow are

$$R_T = \frac{g\alpha\Delta T d^3}{\nu\kappa_T}; \qquad R_S = \frac{g\beta\Delta S d^3}{\nu\kappa_T};$$

$$\sigma = \nu/\kappa_T; \qquad \tau = \kappa_S/\kappa_T;$$

$$Re = \frac{U(d/2)d}{\nu}$$

where the dimensionless mean flow $U(z)$ has been scaled by its velocity at $z = d/2$. In the following, unless explicitly stated, all variables are dimensionless.

The general procedure is to examine solutions of the form

$$\begin{pmatrix} w \\ T \\ S \end{pmatrix} = \begin{pmatrix} w(z) \\ T(z) \\ S(z) \end{pmatrix} \exp i(kx+ly-\omega t), \tag{2.3}$$

where the marginally stable case is given by $\mathscr{R}(\omega) = 0$. For the moment, however, attention will be restricted to stationary disturbances i.e. $\omega = 0$. The solutions (2.3) admit two special cases; transverse modes ($l = 0$) with no variation in the cross-stream direction, and longitudinal modes ($k = 0$) with no downstream variation. These cases will be treated first and then results for a general three-dimensional disturbance will be evaluated on the basis of Squire's transformation.

(b) Longitudinal modes

When $k = 0$, the Eq. (2.1) reduce to those for a two-dimensional disturbance in the absence of shear. This system has been discussed fully by Baines & Gill (1969) who found that perturbations grow when $R^* = R_S - \tau R_T > (27\pi^4/4)\tau$. Hence the basic "no motion" state upon which the perturbations are imposed cannot exist above that value of R^* and it is only relevant to ask whether the shear permits unstable modes for values of R^* less than the critical value found in the absence of shear.

(c) Transverse modes

For these modes $l = 0$; for the sake of simplicity a uniform shear (in dimensional units)

$$U(z) = \lambda z,$$

where $\lambda > 0$ is a constant, is considered: then $Re = \lambda d^2/2\nu$. Consider the case of small shears, i.e. $Re \ll 1$. Then it is anticipated that the variables

may be expanded as a power series in Re as follows:

$$A = A_0 + ReA_1 + Re^2 A_2 + \ldots,$$

for any dependent variable A. The expansion will now be substituted into (2.3) and the equations for different orders of Re examined. (The details of the expansion procedure are given in Appendix 1: all variables referred to here but not defined above are defined in that appendix.)

The 0(1) equations, reduce to those of double-diffusive instability in the absence of shear; the critical value of the effective Rayleigh number R_0^* is

$$R_0^* = R_{S_0} - \tau R_{T_0} = \frac{27\pi^4\tau}{4}.$$

The aim of the following analysis is to determine the effect of the shear on the critical value of R^*. A consideration of the $0(Re)$ equations shows that

$$R_1^* = 0.$$

This result is a necessary consequence of the fact that the stability must be independent of the direction of the shear i.e. the sign of Re. The first correction to R^* comes in at $0(Re^2)$. It is shown in Appendix 1 (Eq. A11) that

$$\frac{R^*}{R_0^*} - 1 = Re^2 C(\alpha_2^2 R_{S_0}^2 + \alpha_1 R_{S_0} + \alpha_0) + 0(Re^4), \tag{2.4}$$

where α_0, α_1, α_2 and C are functions of the wave number k and the molecular properties of the fluid.

Equation (2.4) shows that for the transverse finger modes the effective Rayleigh number required for instability is increased by the presence of shear provided the α's are positive ($R_{S_0} > 0$ for fingers). For the numerical values of σ and τ corresponding to both heat-salt and salt-sugar fingers (in aqueous solutions) the α's are positive. It is possible, however, that for very small values of the Prandtl number σ, α_0 may become negative in which case, under suitable conditions, the transverse modes would be destabilized by the shear. It is interesting to note that the amount of stabilization for a given shear depends on the initial Rayleigh numbers. No further comment on this point will be made here but it will be returned to later when the momentum transfer is considered.

In terms of R^* (2.4) may be written as

$$R^*(k, Re) = R_0^*(k) + Re^2 R_2^*(k) + 0(Re^4).$$

Suppose

$$k = k_0 + Rek_1 + \ldots,$$

then

$$R^*(k, Re) = R_0^*(k_0) + Re^2(\tfrac{1}{2}R_0^{*\prime\prime}(k_0)k_1^2 + R_2^*(k_0)) + 0(Re^4).$$

At k_0,

$$R_0^{*\prime}(k_0) = 0, \qquad R_0^{*\prime\prime}(k_0) > 0.$$

This implies that the best choice of k is k_0 (i.e. $k_1 = 0$) and

$$\min R^*(k, Re) = R_0^*(k_0) + Re^2 R_2^*(k_0) + 0(Re^4).$$

Typical numerical values for heat-salt fingers are $\tau \approx 10^{-2}$, $\sigma \approx 7$ and $R_{S0} \sim 10^5 - 10^8$; then using $k = k_0 = \pi/\sqrt{2}$

$$\frac{R_S - \tau R_T}{27\pi^4\tau/4} - 1 \approx Re^2(10^9 - 10^{15}). \tag{2.5}$$

The large magnitude of the coefficient of Re^2 in (2.5) shows that there is a significant stabilization of the transverse mode even for very small shears. These results are in agreement with some numerical calculations of the linear stability of transverse modes in a constant shear made by Hart (1970). He found that for finite shear rates Re that the modes were stabilized by the shear and that the stabilization occurs at $0(Re^2)$.

(d) A general three-dimensional disturbance

Attention is now returned to the general three-dimensional disturbance described by (2.3). The problem may be reduced to the simpler two-dimensional one by means of Squire's transformation. This transformation states that if Re is the Reynolds number in the x-direction then

$$\bar{k}\bar{Re} = kRe, \tag{2.6}$$

where $\bar{k}^2 = k^2 + l^2$ and $\bar{Re}$ is the Reynolds number of the reduced problem. In this problem the Rayleigh numbers are unaltered, and as $k \leqq \bar{k}$, $\bar{Re} \leqq Re$ and so the three-dimensional perturbation is equivalent to a two-dimensional one with the same R^* but smaller Reynolds number. For longitudinal modes $\bar{Re} = 0$, and hence for any fixed wavenumber they are the most likely to occur.

The above discussion has been restricted to a consideration of stationary disturbances. Now it will be supposed that the phase speed of the disturbance is given by c. Then the linearized equations governing the travelling disturbance are the same as (2.1) except that where z occurs explicitly it is

replaced by $(z-c\,\sigma\,Re)$. As with the other variables write c as a power series in Re. Baines & Gill (1969) showed that in the absence of shear a salt finger mode sets in as a direct instability (in the case of free boundaries). Hence

$$c = Re\,c_1+Re^2c_2+....$$

Fixing attention on the transverse modes it can be shown (see Appendix 2) that $c_n = 0, n = 1, 2, ...$ Therefore for small enough values of the Reynolds number only stationary disturbances are allowed.

(*e*) *Momentum transfer*

The energy equation for the perturbation is (in dimensional units)

$$\frac{\partial}{\partial t}\langle K\rangle = g\,\langle w(\alpha T-\beta S)\rangle-\left\langle uw\frac{\partial U}{\partial z}\right\rangle-\nu\,\langle(\nabla u)^2\rangle\,, \tag{2.7}$$

where K represents the kinetic energy of the perturbation defined by $K = \frac{1}{2}(u^2+v^2+w^2)$, and $\langle\ \rangle$ denotes an average over a volume formed by integrating across the flow in z and over one wavelength in the horizontal. The main concern here is the conversion of mean flow kinetic energy to that of the perturbation by the Reynolds stress term $-\langle uw\rangle\,(\partial U/\partial z)$ (for constant $\partial U/\partial z$). This, in general, will depend on the form of the perturbation; attention is now restricted to the transverse and longitudinal modes. For transverse modes, (again restricting attention to small Re) the above analysis shows that

$$-\langle uw\rangle = -\frac{4Re}{k}\sum_{m\ \text{even}}\frac{m}{m+1}A_m+0(Re^2)$$

where $A_m = (-1)^{-m/2+1}_{a_m}$ is a positive number (see (A.10)). Therefore, for small rates of shear, the Reynolds stress is negative to $0(Re)$ and the transverse modes transfer horizontal momentum vertically against the shear.

For the longitudinal mode it is easily seen that

$$-\langle uw\rangle = \frac{Re}{(n^2\pi^2+l^2)},$$

which is positive. This latter calculation is not dependent on Re being small and it shows that mean flow kinetic energy is converted into perturbation kinetic energy for the longitudinal modes. Similar results were also found by Asai (1970a) for thermal convection at finite shear rates and so by analogy with the thermal problem it seems likely that the transverse mode transfers its energy to the mean flow at finite shear rates in salt finger convection also.

For an arbitrary three-dimensional disturbance set up axes so that the disturbance is described by $w = we^{ikx}$; then the shear has components in two directions $(U(z), V(z), 0)$. There are now two contributions to the Reynolds stress $-\langle uw\rangle$ and $-\langle vw\rangle$. Simple calculations show that the total Reynolds stress may be either positive or negative depending on the orientation of the mode to the shear, and that the total Reynolds stress is zero at an orientation which is independent of the magnitude of the shear.

Finally, it is now possible to see why the stabilization of the transverse mode depends on the value of R_{S_0} (or R_{T_0}). The energy removed from the transverse mode by the Reynolds stress has magnitude

$$-\langle uw\rangle \frac{\partial u}{\partial z} \propto' Re^2 w_0 w_1 ,$$

$$\propto' Re^2 R_{S_0} .$$

This term is not sufficient to account for the stabilization of $0(Re^2 R_{S_0}^2)$ shown in (2.4). A re-examination of the energy equation (2.7) reveals the following feature. The buoyancy term on the right hand side can be written as

$$\begin{aligned} g\langle w(\alpha T-\beta S)\rangle = {} & g\langle w_0(\alpha T_0-\beta S_0)\rangle + Reg\langle w_0(\alpha T_1-\beta S_1) \\ & + w_1(\alpha T_0-\beta S_0)\rangle \\ & + Re^2 g\langle w_1(\alpha T_1-\beta S_1)+w_0(\alpha T_2-\beta S_2)\rangle \\ & + w_2(\alpha T_0-\beta S_0)\rangle + 0(Re^3). \end{aligned}$$

It is easily seen that the term proportional to Re is zero (as must be the case by symmetry). Further $w_2, T_2, S_2 \propto \sin kx$ and so the second and third terms in the equation multiplied by Re^2 are zero. Therefore

$$g\langle w(\alpha T-\beta S)\rangle = g\langle w(\alpha T_0-\beta S_0)\rangle + Re^2 g\langle w_1(\alpha T_1-\beta S_1)\rangle + 0(Re^4)$$

As w_1, T_1 and S_1 are proportional to R_{S_0}, the second term is $0(Re^2 R_{S_0}^2)$, and it is this "buoyancy stress" which arises due to the tilt of the perturbation by the shear that is mainly responsible for the stabilization of the transverse mode.

3. Finite amplitude salt fingers in a uniform shear flow

The linearized stability theory for salt finger modes in a uniform shear flow described in §2 showed that the preferred modes of instability were two-dimensional sheets aligned along the direction of the basic flow. It is pertinent now to ask whether or not these disturbances, which are growing exponentially with increasing time, through modification of the basic velocity, T and S fields can alter their own form to produce a finite equilibrium amplitude, as is the case for two-dimensional rolls in thermal convection. The method of

analysis used here is to expand each dependent variable as a power series in the small, but finite, amplitude of the disturbance in a manner completely analogous to that of Malkus & Veronis (1958). This method of analysis is now quite standard and so will not be reproduced here.

The problem to be solved is identical in geometric form to that of §2. In this case though the full non-linear (Boussinesq) equations are considered; indeed it is the modification of the basic flow by the non-linear terms which allows equilibration of the perturbations. As the previous section showed that as R^* was increased from zero the first mode to become unstable was that of infinite wavelength in the direction of the shear, the investigation is restricted to these modes. All variables are expanded in the form

$$Q = Q_0+\varepsilon Q_1+\varepsilon^2 Q_2+\ldots$$

where ε is the amplitude of the perturbation.

The analysis shows that there is no correction to the effective Rayleigh number at $0(\varepsilon)$: i.e.

$$R_1^* = R_{S_1}-\tau R_{T_1} = 0$$

However, application of the expansion procedure shows that

$$R_2^* = \frac{(l^2+\pi^2)^2}{8l^2\tau}+\frac{(1-\tau^2)}{8\tau(l^2+\pi^2)}R_0^*. \tag{3.1}$$

When $\tau = 1$, this correction reduces to the value found for two-dimensional rolls in thermal convection by Malkus & Veronis (1958). As $\tau \to 0$, $R_2^* \to \infty$ indicating that diffusion of the unstably stratified component is essential for equilibration of these modes. Further,

$$w_2, T_2, S_2 \propto \cos 3\pi z \cos ly,$$

and so the first distortion of the finite amplitude sheet does not effect the plan form but only the vertical structure. The non-dimensional mean profiles of T, S and the velocity are given by

$$\frac{\partial \bar{T}}{\partial z} = 1+\frac{\varepsilon^2}{4(l^2+\pi^2)}\cos 2\pi z,$$

$$\frac{\partial \bar{S}}{\partial z} = 1+\frac{\varepsilon^2}{4\tau(l^2+\pi^2)}\cos 2\pi z,$$

$$\frac{\partial \bar{u}}{\partial z} = 1+\frac{\varepsilon^2}{4(l^2+\pi^2)}\cos 2\pi z, \quad \frac{\partial \bar{v}}{\partial z} = \frac{\partial \bar{w}}{\partial z} = 0. \tag{3.2}$$

The Eqs. (3.2) imply that there are increased gradients near the boundaries whilst for $\varepsilon > 2(l^2+\pi^2)^{\frac{1}{2}}$ the temperature and velocity gradients would become negative in the mid-region of the fluid, and for $\varepsilon > 2\tau(l^2+\pi^2)^{\frac{1}{2}}$ the salinity gradient would reverse.

4. The experimental arrangement

The experiments with sheared salt fingers were carried out in a specially designed channel, which allowed two layers of fluid to be set up in a counter-flow arrangement. The main idea was to allow the salt fingers to form at an interface between these two layers, the shear being produced across the interface by the bulk motion of the layers. For fluids with given molecular properties, salt finger convection depends on the relative values of T and S between the layers (denoted by ΔT and ΔS, respectively). Hence the objective

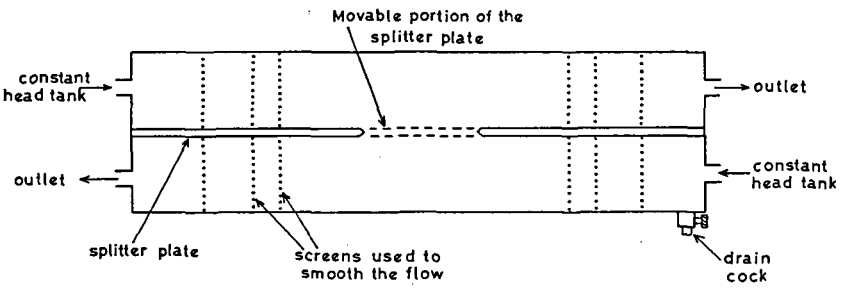

FIGURE 1 A diagrammatic representation of the flow channel.

of these experiments was to compare the properties of the salt fingers for different shear rates, but keeping ΔT and ΔS constant.

The channel is shown diagramatically on Figure 1: the channel was 1.3 m in length and 10×10 cm in cross-section, and was divided into two halves by a horizontal splitter plate running the length of the channel. Thus the flow in each layer was approximately 10 cm wide by 5 cm deep. Unfortunately, for heat-salt fingers the length of the fingers (Linden, 1973) was comparable with the depth of the tank, but in order to avoid this a tank with a volume some ten times the present one would have been required. For sugar-salt fingers, their length was much smaller than the depth of the layer.

At the ends of the channel three wire-mesh screens were placed across the cross-section in order to smooth out the flow. Both sections of the channel were supplied with fluid at given rates controlled by constant-head tanks and

flow meters. As the outflow was discarded it was possible to set up a steady flow by suitably adjusting the outflows. A central portion of the splitter plate could be removed horizontally through one side wall of the tank producing a measurement section of 30 cm in length. This was used to allow the two fluids to come into contact once a basic flow had been set up.

It was found that sugar and salt were the most convenient to use for both qualitative and quantitative purposes. Observations of the plan form of sheared salt-sugar fingers were made using both a shadowgraph and the method of observing the distortions produced to the light paths when a parallel beam was shone through the tank. The latter method was used by Shirtcliffe & Turner (1970) and is described in detail in their paper. Flux estimates were made by measuring the net transport of sugar and salt into the layers by taking bulk samples of the layers at the outlets. This method, which allows the apparatus to average the layers, gives an estimate of the total transport across the interface per unit time. The method of determining the sugar and salt concentrations was to measure the refractive index and the optical rotation of polarized light by the sample. From these two measurements using data from the International Critical Tables it was possible to determine the contributions to the density by the salt and sugar (Shirtcliffe, 1973) to within $\pm 0.03\%$ for sugar and $\pm 0.05\%$ for salt. When the samples were analysed the total salt and sugar content of the two layers was determined. Allowing for the rejection of inconsistent samples it was possible to compare about eight different shear rates for given ΔT and ΔS, before exhausting the supply.

The flux of sugar (and salt) across the interface was determined in the following way. The sugar flux F_S into a stationary layer of depth D is given by

$$F_S = D\frac{dS}{dt},$$

$$= D\left(\frac{S_1 - S_2}{t_1 - t_2}\right),$$

for a constant flux. If the layer is moving with an average velocity $\bar{U}$

$$t_1 - t_2 = L/\bar{U}$$

where L is the length of measurement section. It was found that for all flow velocities used in these experiments that the mean velocity was parabolic.

Consequently, as the initial sugar concentration in the lower layer was zero (i.e. at the inlet)

$$F_S = \frac{Q}{2DL} S \tag{4.1}$$

where S in the sugar concentration at the outlet and Q is the volume flow rate.

Measurements were also made of the vertical fluxes in a heat-salt system. In this case however, the conduction of heat through the splitter plate made accurate measurements extremely difficult. Consequently, in order to avoid this the lower layer was kept stationary throughout these experiments and was sealed off at the ends of the measurement section. Measurements of temperature and salinity were made with a thermistor and a conductivity probe, as described in Linden (1971), accurate to 0.02°C and 0.02%. Two methods of estimating the fluxes were used. In the first, the temperature and conductivity were measured at a point (the centre of the layer) as a function of time and these values were taken to be representative of the whole layer. The fluxes were estimated from the gradients of these curves taking averages over times for which the gradient remained constant (usually about 10 min). The second method used was to stir the lower layer after a run (the splitter plate having been replaced over the measurement section), in order to ensure that the measurements were time averages of the layer. It was found that the two methods produced essentially the same estimates for the fluxes.

The mean flow was measured by means of observing the distortion of dye lines produced by electrically pulsing wires stretched across the tank, with thymol blue solution flowing in the layers (see Linden, 1973). It was found in all cases that the flow was parabolic (within 5%) for all values of the flow rate: the velocity difference between the layers varied from 0–2.0 cm/sec.

Before proceeding to a discussion of the experimental results it is necessary to evaluate one more aspect of the experimental arrangement, namely the effect of the finite measurement section. The finite length of the section has two effects. First, the fingers must develop once the two layers come into contact: calculations of the growth rate of salt fingers (Robinson, 1971) show that for the flow rates used in these experiments the fingers will form approximately 0.1 cm from the edge of the splitter plate. This estimate is in good agreement with observations, and neglect of the region leads to errors of the order of 0.5%.

The second effect of the finite measurement section is that if the two layers are moving with a relative velocity ΔU, then the rate of change of T and S in each layer will vary with change in ΔU even if the actual fluxes across the interface remain unchanged. In the limit $\Delta U \to \infty$, no T or S will cross the interface (in the absence of shear instability and diffusion) as the fluid will be swept away from the measurement section before it can enter the other layer.

It should be emphasised that this is a purely geometrical effect but it must be estimated when considering the fluxes across the interface.

It was shown (Linden, 1973) that the vertical flux of salt across an interface containing salt fingers is proportional to the velocity of the fluid in the fingers. Consider the lower layer to be stationary and the upper layer to be moving with velocity $(U(y, z), 0, 0)$. The salt finger flux into the lower layer will be modelled by considering fluid of depth h, moving with velocity $(0, 0, -w)$. The aim is to determine how much of this fluid is capable of entering the lower layer before being swept past the measurement section by the mean flow. Suppose a parcel of fluid starts at some point (x_0, y_0, z_0) at time $t = 0$. Then at time t its position will be given by $(x_0+\int_0^t U(y_0 z)dt, y_0, z_0-wt)$. Thus for a parcel starting at (x_0, y_0, z_0) to contribute to the flux it is necessary that $z \leqq 0$ for some $x\in[0, L]$ where L is the length of the measurement section. Taking

$$U(y, z) = \lambda z(D-z)(D^2-y^2)$$

where the origin of the coordinate system is the centre of the upstream splitter plate edge, it is easy to show that

$$z^3-\frac{3D}{2}z+\frac{2w(L-x)}{\lambda(D^2-y^2)} = 0, \tag{4.2}$$

is the caustic of a shadow-zone in the tank, above which no parcel can reach the lower layer before being swept from the measurement section. Suppose now that the shear has no dynamical effect on the fingers. Then measurements of the flux obtained from the transports across the interface would decrease as λ increases. This decrease, due to more of the fluid being in the shadowzone, is given by

$$J = \frac{1}{2LDh}\int_o^L\int_{-D}^{D} z(x, y)dx\,dy, \tag{4.3}$$

where $z(x, y)$ is the solution to (4.2) provided $z \leqq h$. If $z > h$ (the length of the fingers) then it is replaced by h in the integration. In other words, the volume under the shadowzone is calculated up to a height determined by the length of the fingers.

There are uncertainties in estimating J for a particular situation: for heat-salt runs w was estimated on the basis of the data given in Linden (1973) and h was taken to be the depth of the layer. For the sugar-salt runs h was determined from a shadowgraph and the velocity and "guessed" on the basis of a scale analysis.

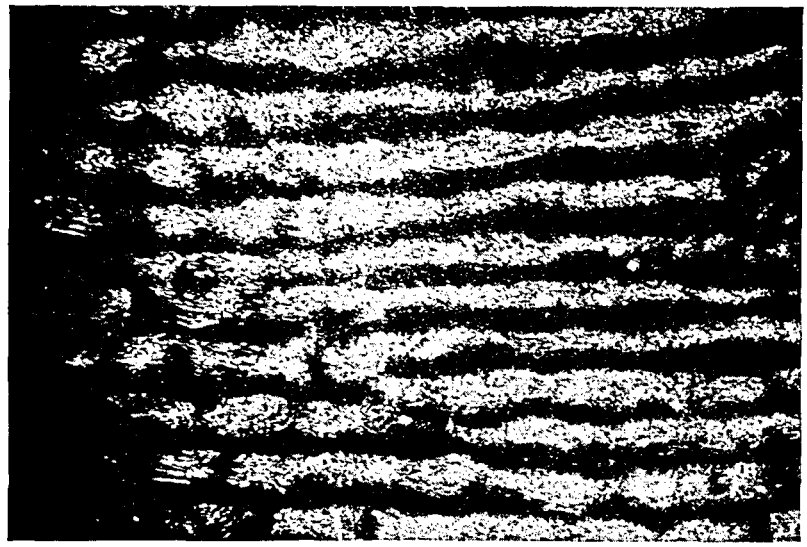

a

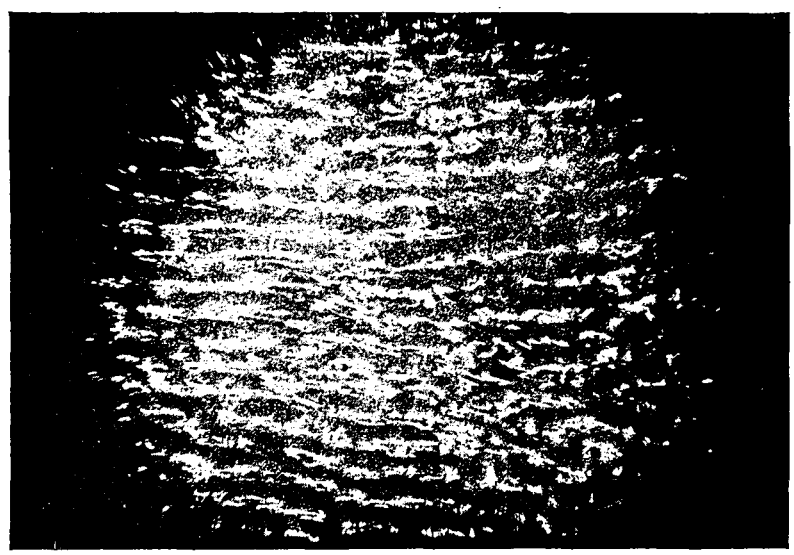

b

FIGURE 2 Plan view of two-dimensional sheets; the mean flow is horizontal in these photographs.

5. The experimental results:

(1) Qualitative Observations of Sugar-salt Fingers

Although it was possible to visualise both the horizontal and vertical structure of the fingers with a shadowgraph the observations of the plan form gave the most information. The use of a shadowgraph in viewing the vertical structure is limited by the fact that the resulting patterns are the sum of all deviations along a horizontal light path. As the mean flow varied in the horizontal, with the velocity being zero on the side walls the fingers in these relatively shear free areas obscure the structure in the centre of the tank. However certain features could be ascertained.

For all flow rates used, strong convective motion was observed in both layers on either side of a distinct interface region of some 0.5–1.5 cm in thickness. Buoyant elements were observed to break off from this interface and be swept downstream by the mean flow; the break off process appeared to be identical in form to that reported for unsheared fingers (Stern & Turner, 1969, Shirtcliffe & Turner, 1970). The interface appeared to become thinner with increasing flow rates, but was constant in thickness over the majority of the measurement section, the ends of the splitter plate affecting the motion for 1–2 cm downstream.

Observations of the plan form, either with a shadowgraph or using the method of Shirtcliffe & Turner (1970), indicated the following change in patterns as the shear increased. When there was no shear the observed plan form is that of essentially square cells with arbitrary orientation (see Shirtcliffe & Turner (1970) for some excellent photographs). As the shear is increased the first effect is an immediate alignment of these cells into rows parallel to the mean flow; this alignment was observed at all values of ΔU (the velocity difference between the centres of the layers) except zero; the lowest value attained in these experiments was 0.04 cm/sec. As the magnitude of the shear increased the cells were elongated in the downstream direction. Further increase of the shear removed any visible variation in the downstream direction. Figure 2 shows two examples of these two-dimensional sheets shown in plan form.

At no stage was it possible to inhibit the formation of these longitudinal sheets by the shear, although the smallest value of an overall Richardson number $Ri = g\Delta\rho D/\rho_0(\Delta U)^2$, where $\Delta\rho$ is the density step across the interface, obtained was 6.2. This value of Ri was the limit of the controlled experiments. During filling it was possible to get lower Richardson numbers and up until mixing occurred the two-dimensional mode structure was visible. It is clear that if the shear tilted the fingers from the vertical, the plan view would also show two-dimensional sheets. However, viewing the plan form using

light at angles up to 60° to the vertical failed to reveal any cross-stream structure.

(2) Quantitative Results

(a) Stabilization of the transverse mode of sugar-salt fingers

In §2 it was shown that the shear stabilizes all modes which have a component of the shear normal to their wavecrests. It is convenient to rewrite (2.4) as

$$\lambda \propto \left(\frac{R^*-R_0^*}{R_0^*}\right)^{\frac{1}{2}} C^{-\frac{1}{2}}(\alpha_2 R_{S_0}{}^2+\alpha_1 R_{S_0}+\alpha_0)^{-\frac{1}{2}}.$$

Hence the value of the shear λ_c at which transverse mode is suppressed is related to $\alpha\Delta T$ and $\beta\Delta S$ by

$$\lambda_c \propto \frac{(\beta\Delta S-\tau\alpha\Delta T)^{\frac{1}{2}}}{\alpha\Delta T} \tag{5.1}$$

provided $R^* \gg R_0^*$ (as was the case in the experiments). λ_c was determined experimentally by observing the plan form with a shadowgraph and increasing the flow rate until the transverse modes disappeared and only sheets aligned downstream remained. Then, by dropping dye crystals into the tank, the shear across the interface was determined from photographs. A series of runs was carried out in which $\alpha\Delta T$ varied between 10–33% and $\beta\Delta S/\alpha\Delta T$ from 0.4–0.9. The results of the determination of λ_c shown on Figure 3 are well correlated by the relationship (5.1).

(b) Sugar-salt flux measurements

The fluxes of sugar and salt across the interface are shown on Figure 4. These plots show the fluxes normalised with respect to the value of the flux at zero shear, as a function of the velocity difference between the layers. The four runs shown span a range of $0.015 \leqq \alpha\Delta T \leqq 0.074$ and $0.014 \leqq \beta\Delta S \leqq 0.044$, and were chosen because of their completeness of data points over the range of ΔU. There is a considerable scatter on the results but note that there is an increase in the flux as the velocity difference increases. This increase is greater in the sugar flux than in the salt flux, a trend which is reflected in the fact that the ratio of the fluxes $r = F_T/F_S$ decreases with increasing ΔU (Figure 5).

(c) Heat-salt flux measurements

The increase in salinity and temperature of the lower layer as functions of time are shown on Figures 6 and 7. These curves, which are representative of the data, show that as ΔU increases the salt transport into the layer decreases,

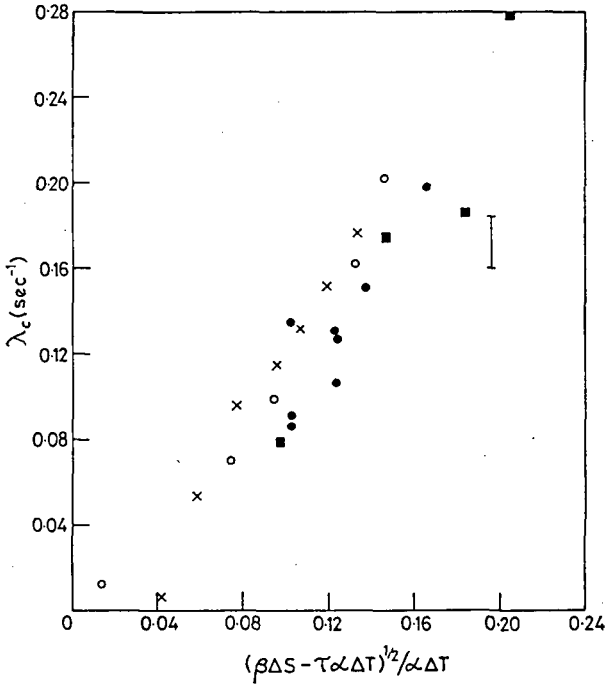

FIGURE 3 The value of the shear λ_c which stabilizes the transverse mode plotted against $(\beta\Delta S - \tau\alpha\Delta T)^{\frac{1}{2}}/\alpha\Delta T$. The error bars indicate an estimate for the uncertainty in determining λ_c.

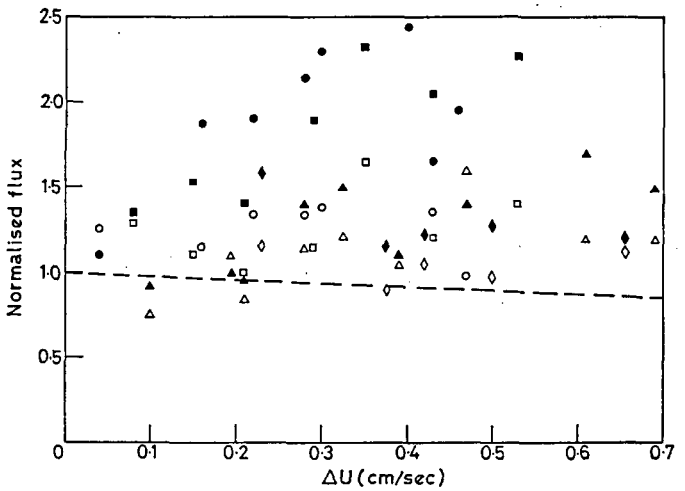

FIGURE 4 The fluxes of sugar and salt, normalised with respect to the value at zero shear, plotted against the velocity difference ΔU. There are four values of $\alpha\Delta T$ and $\beta\Delta S$ represented here: $\alpha\Delta T = 18.0‰$, $\beta\Delta S = 15.0‰$—●: $\alpha\Delta T = 37‰$ $\beta\Delta S = 21.0‰$—■: $\alpha\Delta T = 74.0‰$, $\beta\Delta S = 44.0‰$—▲ $\alpha\Delta T = 15.0‰$, $\beta\Delta S = 14.0‰$—◆. Closed symbols refer to the sugar flux and open ones to the salt flux. The broken line represents the flux reduction due to the shadowzone when $w = 0.01$ cm/sec and $h = 1.5$ cm.

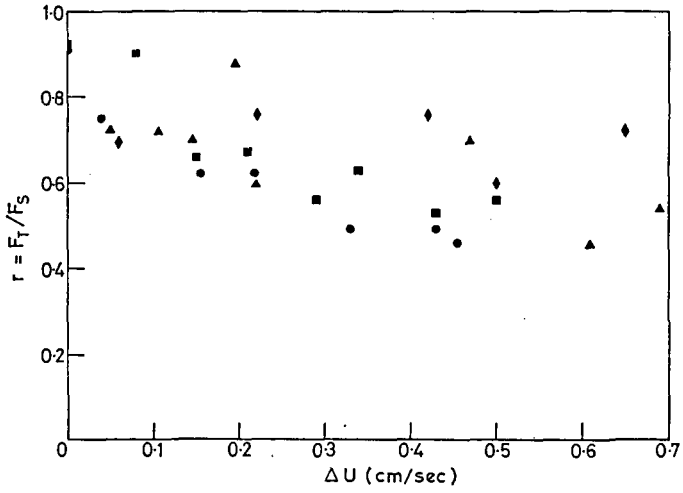

FIGURE 5 The ratio of the buoyancy fluxes r plotted against ΔU. The symbols have the same meaning as those referred to in the caption to figure 4.

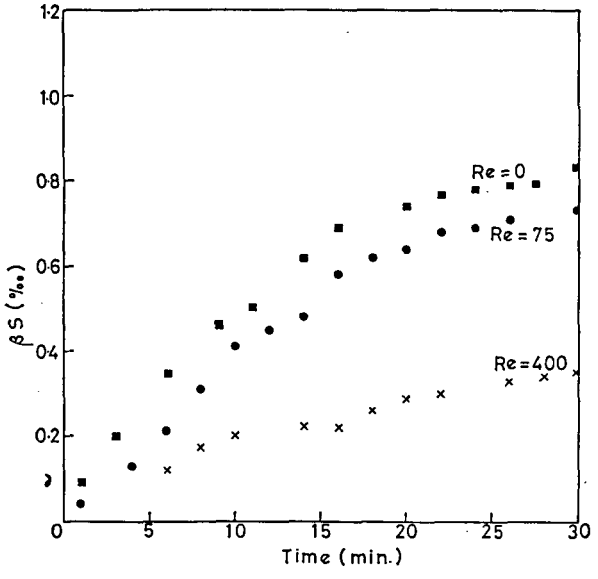

FIGURE 6 The increase in salinity of the lower layer for various values of Re plotted against the time measured from the time of withdrawal of the central portion of the splitter plate.

whereas the heat transport decreases initially and then increases with further increases in ΔU. The normalised salt fluxes are shown on Figure 8 and the normalised heat fluxes on Figure 9: the points marked with an open symbol denote values obtained by stirring the lower layer before and after the measuring period. They were used as a check on the validity of using a point reading

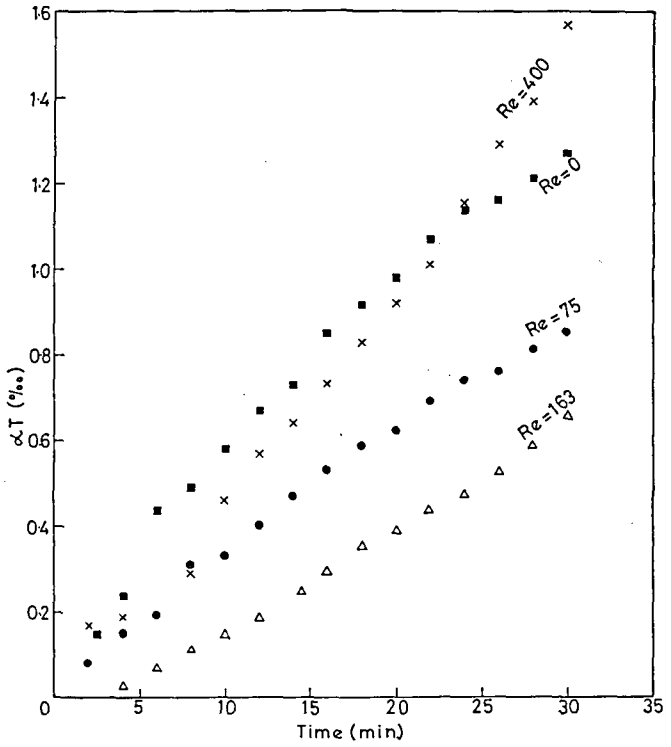

FIGURE 7 The increase in temperature of the lower layer corresponding to the salinity increase shown on figure 6.

to represent an average layer value; the agreement between the fluxes determined these two ways is taken as a justification of the method.

6. Discussion of the experimental results

The fluxes of sugar and salt are seen to increase with increasing shear. For sugar-salt fingers the shadowzone effect is small, implying a decrease in flux of approximately 10% over the range in ΔU used in the experiments. The

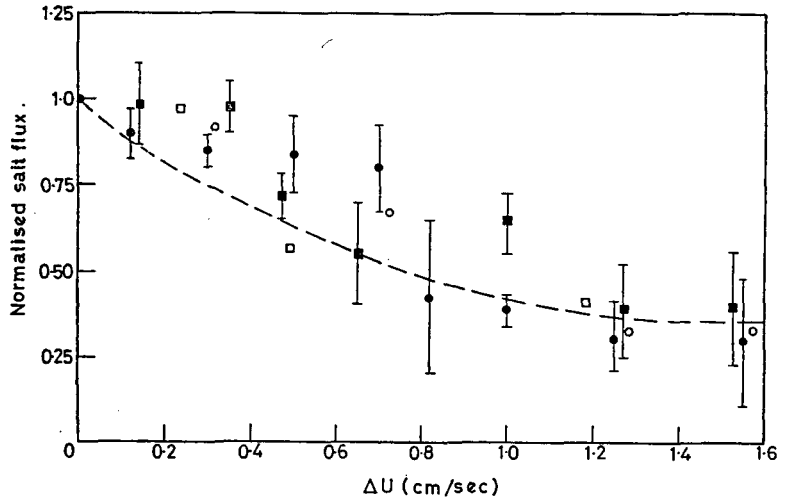

FIGURE 8 Normalised salt fluxes plotted against ΔU. $\alpha\Delta T = 3.5 \pm 0.4‰$, $\beta\Delta S = 0.7 \pm 0.15‰$—● $\alpha\Delta T = 2.6 \pm 0.4‰$, $\beta\Delta S = 0.4 \pm 0.1‰$—■. The broken line represents the flux reduction due to the shadowzone when $w = 0.05$ cm/sec.

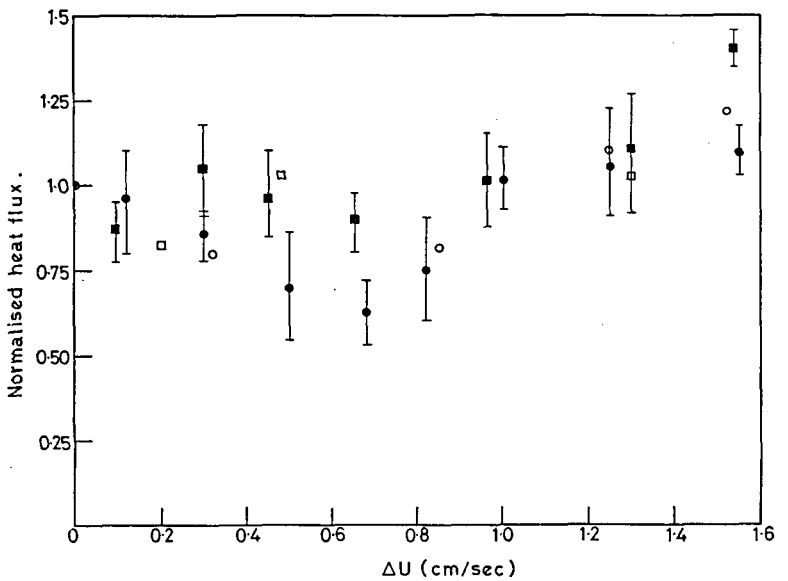

FIGURE 9 The normalised heat flux corresponding to the salt fluxes for the parameters shown on figure 8.

decrease in flux due to the shadowzone, based on a velocity of 0.01 cm/sec and an interface thickness of 1.5 cm is shown on Figure 4: this curve then represents the flux which would be measured if the shear had no dynamical effect on the fingers. The observed increase in flux with increasing ΔU is consistent with the notion that unsheared salt fingers are in a state of "quasi-equilibrium" (Linden, 1973) with the flux through the fingers being equal to that into the convecting layers on either side. In these experiments the mean flow advects sugar and salt away from the interface region, thereby increasing the potential of the convecting regions to take a larger flux from the fingers. This idea is borne out by the observations that the interface becomes thinner with increasing shear, thereby increasing the gradients across the interface; unfortunately, a systematic study of interface thickness was not made. This increase in flux resulting from the horizontal advection will only occur when there are horizontal inhomogeneities in the layers (as was the case in the experiments). In oceanic situations where large scale homogeneous layers are found (see, e.g. Tait & Howe, 1971) this effect will not be relevant.

The fact that the sugar flux increases at a rate greater than the increase in salt flux as ΔU increases is indicated by the fact that r decreases from 0.92 at $\Delta U = 0$ to about 0.6 at $\Delta U = 0.7$ cm/sec. In a manner not yet properly understood unsheared salt fingers adjust so that r is constant over a large range of $R_\rho = \alpha\Delta T/\beta\Delta S$. Any distortion of the length and shape of the fingers is almost certain to change the diffusion balance in the fingers and so cause a change in r. However, it is not clear how the value of r depends on the shape of the fingers or indeed on the dynamics of the transition between the well-ordered finger motions and the convecting layers.

The heat-salt transports across the interface exhibit similar features to the sugar-salt case. It must be remembered that the shadowzone effect is more important for heat-salt fingers: for example, based on a finger velocity of 0.05 cm/sec and assuming the fingers reach to the top of the tank, then the reduction in measured transport is approximately 60% when $\Delta U = 1.6$ cm/sec. The shadowzone reductions are indicated by the broken line on Figure 8. In view of this calculation, the measurements show that the flux of salt through the fingers is virtually unaffected by the shear. In this case the depth of the tank is insufficient to allow a quasi-equilibrium situation to be set up and the increase in flux due to advection by the mean flow is not found. Therefore, it is concluded that a steady shear does not inhibit the salt flux across the interface, the two-dimensional sheets being as efficient transporters of salt as the salt fingers. This result is to be contrasted with the conclusion that turbulent motions, by their disruption of the fingers, do inhibit the salt flux (Linden, 1971).

The heat flux measurements show a trend similar to those of the salt flux, except that at large ΔU the flux increases again. It seems likely that this

increase in flux is due to conduction across the interface as the temperature gradients are sharpened at the splitter plates as ΔU increases. However this explanation is at best tentative and needs more investigation before it can be verified.

7. Conclusions

The work described in this paper attempts to determine whether or not salt fingers can exist in the presence of steady shear flows. As the main motivation was to see whether oceanic microstructure, which very likely supports velocity shears, can in some circumstances be produced by salt finger convection, the study has concentrated on determining whether or not the influence of salt fingers is inhibited by shear. Linear stability analysis for small shears revealed that all modes with a component of the shear normal to their wavecrests are inhibited by the shear, and that the preferred mode of instability is a two-dimensional mode parallel to the mean flow. The finite amplitude properties of these modes was then investigated by the procedure of making an expansion in the perturbation amplitude ε. It was shown that the sheets were stable to $0(\varepsilon^3)$, and that the first finite amplitude correction only effects the vertical structure and not the horizontal plan form.

The experiments showed that the fingers were first aligned by the shear, and then as the shear was increased the transition to the two-dimensional sheets was observed. Estimates of the vertical fluxes of S and T across the interface indicated that the fluxes were not significantly reduced by the shear. The two main properties of the salt fingers which have a particular relevance to the ocean are the large (compared with diffusive fluxes) vertical fluxes of S and T carried by the fingers and the ability of the fingers to produce layered S and T structure. Layering is produced (Turner, 1967) by the unstable buoyancy flux $gF_S(1-r)$ across the interface which can mix the fluid on either side. The experiments have been restricted to the case where the interface is stable to shear instability. Within this restriction it is concluded that a steady shear transforms the salt fingers into two-dimensional sheets which also produce large S and T fluxes in the vertical. Further, as r decreases with increasing shear the unstable buoyancy flux across the interface increases, thereby enhancing the potential of the fingers to produce layered microstructure from initially smooth gradients. This conclusion is in contrast to the observations that unsteady shears (turbulence) inhibit the flux and the ability of the fingers to produce layered structure (Linden, 1971).

The experiments indicate that in the ocean the fingers will be aligned in the direction of any mean currents. Consequently, by designing an instrument which can detect the direction of the current the relative orientation of the instrument and the fingers will be known. This is particularly important if the

array structure of the finger is to be used as an aid to their detection, as is the case with some optical methods. Also, in the ocean, there will almost certainly be some feedback between the salt fingers (if they exist) and the shear. In these situations the scale of the larger motions may be so large that Coriolis effects may be important. However, the results of this investigation indicate that salt fingers may play a significant role in the vertical transport of heat and salt in some areas of the ocean, even if significant velocity shears are present.

ACKNOWLEDGEMENTS

I wish to thank Dr. J. S. Turner for suggesting this problem to me and for many stimulating discussions during the progress of this work. The project was supported by a grant from the Natural Environment Research Council.

Appendix 1

THE EXPANSION PROCEDURE FOR SMALL *Re*

For the transverse mode the 0(1) equations may be written as

$$L(w_0) = 0 \tag{A1}$$

where L is a linear operator of the form

$$L \equiv ABC\nabla_2^2 + (R_{T_0}C - R_{S_0}B)\frac{\partial^2}{\partial x^2},$$

where

$$A \equiv \frac{1}{\sigma}\left(\frac{\partial}{\partial t} - \nabla_2^2\right); \quad B \equiv \left(\frac{\partial}{\partial t} - \nabla_2^2\right); \quad C \equiv \left(\frac{\partial}{\partial t} - \tau\nabla_2^2\right); \quad \nabla_2 = \frac{\partial^2}{\partial x^2} + \frac{\partial^2}{\partial z^2}.$$

For stationary disturbances, the marginally stable case is given by $\partial/\partial t \equiv 0$ and the well known solution is

$$\begin{bmatrix} w_0 \\ T_0 \\ S_0 \end{bmatrix} = \begin{bmatrix} 1 \\ -\dfrac{1}{(k^2+m^2\pi^2)} \\ -\dfrac{1}{\tau(k^2+m^2\pi^2)} \end{bmatrix} \cos kx \cos m\pi z, \tag{A2}$$

m integral, with

$$R_0^* = R_{S_0} - \tau R_{T_0} = \tau(k^2 + m^2\pi^2)^3/k^2 \tag{A3}$$

The most unstable mode has $k^2 = \pi^2/2$, $m = 1$ when $R_0^* = (27\pi^4/4)\tau$. The $0(Re)$ equations are

$$\begin{aligned} L(w_1) = &-\frac{z}{\sigma} BC\nabla_2^2 w_{0x} + zR_{S_0} BS_{0xxx} - zR_{T_0} CT_{0xxx} \\ &+ BC(R_{T_1} T_{0xx} - R_{S_1} S_{0xx}), \\ \equiv &\, f \end{aligned} \tag{A4}$$

where L is as in (A1). A necessary condition for the existence of a non-trivial solution to this problem is

$$\int_\Omega w_0 f \, d\Omega = 0 \tag{A5}$$

where f is the forcing function (the r.h.s. of (A4)) and Ω is the gap in z times one wavelength in x. Application of (A5) to (A4) gives (after substitution of (A2))

$$\frac{R_{T_1}}{R_{S_1}} = \tau; \quad \text{i.e.} \quad R_1^* = 0. \tag{A6}$$

It is thus necessary to go to $0(Re^2)$ to determine the correction to R_0^*. To this order the equations may be written as

$$L(w_2) = F(w_0, w_1, T_0, T_1, S_0, S_1, R_{T_0}, R_{T_1}, R_{T_2}, R_{S_0}, R_{S_1}, R_{S_2}). \tag{A7}$$

Application of (A5) to (A7) gives

$$\begin{aligned} R_{T_2} \int_{-\frac{1}{2}}^{\frac{1}{2}} dz \int w_0 BCT_{0xx} dx - R_{S_2} \int_{-\frac{1}{2}}^{\frac{1}{2}} dz \int w_0 BCS_{0xx} \, dx \\ = \int_{-\frac{1}{2}}^{\frac{1}{2}} dz \int w_0 \Big\{ zR_{T_0} CT_{1xxx} - zR_{S_0} BS_{1xxx} + \frac{z}{\sigma} BC\nabla_2^2 w_{1x} \\ - R_{T_1} BCT_{1xx} + R_{S_1} BCS_{1xx} \Big\} dx. \end{aligned} \tag{A8}$$

In order to solve for R_{T_2} and R_{S_2} it is necessary to find w_1, T_1 and S_1 from (A4). For $m = 1$, one has

$$\nabla_2^6 w_1 + b^2 w_{1xx} = az \sin kx \cos \pi z, \tag{A9}$$

where

$$a = -\left(\frac{k(k^2+\pi^2)^2}{\sigma} + k^3 \left(\frac{R_{S_0}}{\tau} - R_{T_0} \right) \Big/ \left(k^2 + \pi^2 \right) \right),$$

$$b^2 = (\tau R_{T_0} - R_{S_0})/\tau.$$

The boundary conditions on w_1 are

$$w_1 = w_{1zz} = w_{1zzzz} = 0, \quad \text{on} \quad z = \pm\tfrac{1}{2}.$$

The solution of (A9) may be written in the form

$$\begin{pmatrix} w_1 \\ T_1 \\ S_1 \end{pmatrix} = \sum_{m \text{ even}} \begin{pmatrix} a_m \\ b_m \\ c_m \end{pmatrix} \sin m\pi z \sin kx \tag{A10}$$

where

$$a_m = -\frac{8a(-1)^{m/2-1}(m^2+1)}{\pi^2(m-1)^2(m+1)^2[(m^2\pi^2+k^2)^3+b^2k^2]},$$

$$b_m = -\frac{1}{(m^2\pi^2+k^2)}\left\{a_m + \frac{8k(-1)^{m/2}(m^2+1)}{\pi^2(k^2+\pi^2)(m-1)^2(m+1)^2}\right\},$$

$$c_m = -\frac{1}{\tau(m^2\pi^2+k^2)}\left\{a_m + \frac{8k(-1)^{m/2}(m^2+1)}{\tau\pi^2(k^2+\pi^2)(m-1)^2(m+1)^2}\right\}.$$

In order to obtain estimates for R_{T_2} and R_{S_2} using (A10) the series is truncated. As $a_m = 0(m^{-8})$, $b_m = 0(m^{-4})$ and $c_m = 0(m^{-4})$ the series is truncated after one term, i.e. $m = 2$. Substitution of $w_0, w_1, T_0, T_1, S_0, S_1$ in (A8) gives

$$\frac{R^*}{R_0^*} - 1 = Re^2 C(\alpha_2 R_{S_0}^2 + \alpha_1 R_{S_0} + \alpha_0) + 0(Re^4), \tag{A11}$$

where

$$C = 2^7 \cdot 10^2/(3^5\pi^8\tau k^2 N),$$

$$\alpha_2 = k^3(1-\tau)^2/NL\tau^3,$$

$$\alpha_1 = \frac{(1-\tau)}{\tau}\left(\frac{kN^2}{\sigma L} + \frac{27\pi^4}{4}\frac{k^3}{NL}\right) + \frac{(1-\tau)k^3}{\tau^2 NL}\left(\frac{27\pi^4}{4}\tau k^3 - \frac{\tau}{\sigma}kM^3\right) + \frac{k^4}{\tau^2 N}(1-\tau^2),$$

$$\alpha_0 = \left(\frac{27\pi^4}{4}\tau k^3 - \frac{\tau}{\sigma}kM^3\right)\left(\frac{kN^2}{\sigma L} + \frac{27\pi^4}{4}\frac{k^3}{NL}\right) + \frac{27\pi^4}{16}k^4\tau,$$

$$L = M^3 + b^2k^2, \quad M = 4\pi^2 + k^2, \quad N = k^2 + \pi^2.$$

Appendix 2

PROOF OF STATIONARY DISTURBANCES

Assume that the limit $Re \to 0$ is not singular. Then (Baines & Gill, 1969) for $Re \ll 1$ expand the phase speed c of a disturbance as

$$c = c_1 Re + c_2 Re^2 + \dots . \tag{A12}$$

Attention is fixed on the transverse mode, noting that the result for a three-dimensional disturbance follows (see §2(d)) by Squire's transformation. In general now R^* will be complex: in order that the result be physically meaningful R^* must be real which is sufficient to determine c.

The terms proportional to Re now give applying the solubility condition (A5) to (A4) (in place of (A6)).

$$R_1^* + ic_1 G(w_0, T_0, S_0, R_{T_0}, R_{S_0} = 0), \tag{A13}$$

where G is a known function consisting of integrals of w_0, T_0, S_0, R_{T_0} and R_{S_0}. The real part of (A13) implies $R_1^* = 0$ as before: the imaginary part (as w_0, T_0, S_0 are even functions of z and therefore $G \neq 0$) implies that $c_1 = 0$. Suppose now that $c_m = 0$ for $m = 0, \dots, n$. Then to $0(Re^{n+1})$ it is easily seen that the equations may be written in the form

$$L(w_{n+1}) = F(w_j, T_j, S_j, R_{T_j}, R_{S_j}, R_{S_{n+1}}, R_{T_{n+1}}) + ic_{n+1} G(w_0, T_0, S_0, R_{S_0}, R_{T_0}) \qquad j = 1, \dots, n$$

where F and G are known. Application of (A5) gives

$$\int_\Omega (F + ic_{n+1} G) w_0 d\Omega = 0.$$

Equating real parts of this equation gives the condition on R_{n+1}^* and equating imaginary parts with the condition that R^* is real gives $c_{n+1} = 0$ as w_0, T_0, S_0 are even functions of z. Hence, by induction, $c_n = 0$ for all n.

REFERENCES

Asai, T., "Cumulus convection in the atmosphere with vertical wind shear: Numerical experiment," *J. Meteor. Soc. Japan* **42**, 245–259 (1964).

Asai, T., "Three dimensional features of thermal convection in plane Couette flow," *J. Meteor. Soc. Japan* **48**, 18–29 (1970a).

Asai, T., "Stability of plane parallel flow with variable vertical shear and unstable stratification," *J. Meteor. Soc. Japan* **48**, 129–138 (1970b).

Baines, P. J. and Gill, A. E., "On thermohaline convection with linear gradients," *J. Fluid Mech.* **34**, 289–306 (1969).

Chandra, K., "Stability of fluids heated from below," *Proc. Roy. Soc.* A **164,** 231–242 (1938).

Deardorff, J. W., "Gravitational instability between horizontal plates with shear," *Phys. of Fluids* **8,** 1027 (1965).

Gallagher, A. P. and Mercer, A.," On the behaviour of small disturbances in plane Couette flow with a temperature gradient," *Proc. Roy. Soc.* A **286,** 117–128 (1965).

Graham, A., "Shear patterns in an unstable layer of air," *Phil. Trans. Roy. Soc.* A **714,** 285–296 (1934).

Hart, J. E., "Thermal convection between sloping boundaries," Ph.D. thesis, *M.I.T.* (1970).

Ingersoll, A. P., "Thermal convection with shear at high Rayleigh number," *J. Fluid Mech.* **25,** 209 (1966a).

Ingersoll, A. P., "Convective instabilities in plane Couette flow," *Phys. Fluids* **9,** 682–689 (1966b).

Jeffreys, A., "Some cases on instability in fluid motion," *Proc. Roy. Soc.* A **118,** 195–208 (1928).

Kuo, H. L., "Perturbations of plane Couette flow in a stratified fluid and the origin of cloud sheets," *Phys. of Fluids* **6,** 195–211 (1963).

Linden, P. F., "Salt fingers in the presence of grid-generated turbulence," *J. Fluid Mech.* **49,** 611–624 (1971).

Linden, P. F., "On the structure of salt fingers," *Deep-Sea Res.* **20,** 325–340 (1973).

Malkus, W. V. R. and Veronis, G., "Finite amplitude cellular convection," *J. Fluid Mech.* **4,** 225 (1958).

Robinson, J. L., *Thermohaline convection* (Unpublished manuscript) (1971).

Shirtcliffe, T. G. L., "Transport and profile measurements of the diffusive interface in double diffusive convection with similar diffusivities" *J. Fluid Mech.* **57,** 27–43 (1973).

Shirtcliffe, T. G. L. and Turner, J. S., "Observations of the cell structure of salt fingers," *J. Fluid Mech.* **41,** 707 (1970).

Stern, M. E. and Turner, J. S., "Salt fingers and convecting layers," *Deep-Sea Res.* **16,** 491–511 (1969).

Tait, R. I. and Howe, M. R., "Some observations of thermohaline stratification in the deep ocean," *Deep-Sea Res.* **15,** 275–280 (1968).

Tait, R. I. and Howe, M. R., "Thermohaline staircase," *Nature* **23,** 179 (1971).

Turner, J. S., "Salt fingers across a density interface," *Deep-Sea Res.* **14,** 599–611 (1967).